Surface Renewal Estimates of Scalar Exchange

By Kyaw Tha Paw U[1], Richard L. Snyder[1], Donatella Spano[2], and Hong-Bing Su[3]

[1]Department of Land, Air and Water Resources
University of California
Davis, CA 95616

[2] Universita' della Basilicata
Via Nazario Sauro, 85
85100 Potenza - Italy

and

Università di Sassari
Dipartimento di Economia e Sistemi Arborei
Via De Nicola, 1
07100 Sassari - Italy

[3] Atmospheric Science Program
Department of Geography
Indiana University
120 Student Building
701 East Kirkwood Avenue
Bloomington, IN 47405-7100

1. Introduction

The plant canopy-atmosphere exchanges of heat, water vapor, carbon dioxide, and other trace materials are critical topics in plant biometeorology. Evapotranspiration and the ecosystem-atmospheric carbon balance are two ubiquitous examples of plant canopy-atmosphere exchange. Therefore, the development and refinement of practical and inexpensive measurement and estimation techniques of such canopy-atmosphere exchanges is very important.

The surface-atmosphere exchange of scalars (such as heat, water vapor, carbon dioxide, other trace gases, particulates), and vectors (momentum) has been measured and estimated using a variety of techniques. These include eddy-covariance (Swinbank 1951; 1955), the eddy-accumulation method (Desjardins, 1972), gradient-micrometeorological methods (Thornthwaite and Holzman, 1942; Pasquill, 1950; Inoue et al., 1958; Lemon, 1960; Munn, 1961; Pruitt, 1963), horizontal mass flux (advection) (Denmead et al., 1977) and the Bowen-ratio Energy Budget (BREB) method (Sutton, 1953; Tanner, 1960; Pruitt and Lourence, 1968; Denmead and McIlroy, 1970, Verma et al., 1978). These conventional methods have been in development and use for several decades, and generally require complex, expensive measurements.

All of these methods require data logging capable of logging a range of acceptable frequencies; inexpensive modern dataloggers are now readily available for this task; however, the number and type of sensors differ for each method. In the eddy-covariance method, high frequency logging (e.g., 8-10 Hz or higher) is needed for the three dimensional velocity field and the scalar of interest. This generally requires sonic anemometry, which is both relatively complicated and expensive. The scalar must also be sampled with costly, complex sensors at similar frequencies. For temperature, however, either the sonic-based temperature (Paw U et al., 2000) or simple, inexpensive temperature sensors such as thermocouples are used. In the eddy-accumulation methods, and the relaxed eddy-accumulation, sampling of the scalar is made conditionally based on the vertical velocity signal. This reduces the necessity for high-frequency scalar measurements.

In micrometeorological methods, which depend on the measurements of gradients, such as the Bowen Ratio Energy Budget (BREB), advective, or flux-gradient methods, carefully matched and calibrated sensors are needed. In addition, other requirements and limitations exist for each of these methods. To obtain the sensible heat flux density, the BREB requires measurements of the ground heat flux, biomass storage, and net radiation, and two pairs of high-resolution matched temperature and humidity measurements. Under some conditions, small errors in the matched pair measurements can result in large errors of sensible and latent heat flux density. Also, large errors in latent heat flux density can occur near sunrise and sunset when the Bowen ratio $\beta = H/\lambda E \approx -1.0$. The surface is assumed to be horizontally homogeneous, resulting in only vertical transport.

For horizontal and vertical advective-gradient methods several sets of matched sensor pairs are needed. Again, small errors in the matched sensor measurements can result in large flux density estimation errors. Vertical flux-gradient methods require at least one pair of matched scalar sensors and several wind speed measurements to obtain estimates of the vertical turbulent transport coefficients. Similarity or a wind profile coupled with some similarity assumptions is sometimes assumed to assist in obtaining the coefficients. Again, horizontal homogeneity is assumed as in BREB, and errors in the matched sensors or departures from similarity result in potential flux estimation errors.

Paw U and Brunet (1991) introduced a novel method for estimating scalar fluxes based on surface renewal concepts. The paradigms were based on observations of canopy turbulence and the time-space scalar field associated with identifiable, repeated, spatially extensive 'turbulent coherent structures.' Subsequently, several research groups have further developed the method. This chapter reviews the basic theories of surface renewal, and the applications to flux measurements, and a discussion on future developments.

2. Literature Review

2.1 Chemical Engineering: The Beginning

The concept of surface renewal was originally developed in the chemical engineering literature, and it is considered an abstraction and simplification of the later-developed 'transilient' paradigm elucidated by Stull (1984; 1988) for the atmosphere. Higbie (1935) described the transport of gasses to liquids. Liquid elemental volumes, with some scalar value characteristic of the outer liquid layers, were hypothesized to come into contact with the surface-gas interface for fixed time intervals, and then be turbulently removed from the surface. During this contact time, molecular diffusion transferred the gas into the liquid. Standard analytical diffusion equation solutions were used to estimate the transfer during this contact time. The liquid elemental volumes were assumed of semi-infinite dimensions, simplifying these analytical solutions.

Danckwerts (1951) introduced the idea of a variable time interval. Later the concept that there was a quiescent liquid layer at the surface separating the renewed fluid elemental volumes and the surface was added (Danckwerts, 1955). Dobbins (1956) and Torr and Marchello (1958) added finite elemental volume to the surface renewal concept. The method was also applied to vector (momentum) transport (Einstein and Li, 1956). Eddy statistics for surface renewal were postulated by Perlmutter (1961). Subsequent developments included abstracting the process to the fluid elemental volumes approaching at random distances from the surface, for random time intervals (Harriott, 1962), and other studies (Koppel et al., 1966; Bullin and Dukler, 1972)

In the next few decades, numerous applications and modifications to the original technique were published in the engineering literature. These include transient flow concepts (Chung et al., 1971), and momentum transfer applications (Meek and Baer, 1970; Disrud and Fan, 1976). More recent papers include those from Brodkey et al. (1978), Komori et al. (1982; 1989), Khan (1990), Asher and Pankow (1991), Koltuniewicz (1992), Yuan and Liburdy (1992), Musschenga et al, (1992), Fan et al. (1993), Zudin (1993), Yoon and Park (1994; 1995), Koltuniewicz and Noworyta (1994), Pence et al. (1994), and Shimada et al. (1998). The engineering method has also been applied to the ocean surface-atmosphere interface (Phillips, 1992; Soloviev and Schussel, 1994; Clayson et al., 1996; Zappa et al, 1998).

2.2 Plant Canopy Turbulence

Current paradigms of turbulence near plant canopies are based on the dominance of turbulent coherent structures, analogous to such structures reported in the engineering literature (Kline et al., 1967; Offen and Kline, 1974; Chen and Blackwelder, 1978; Rajagopalan and Antonia, 1981 Johansson and Alfredsson, 1982; Bogard and Tiederman, 1986,1987; Talmon et al., 1986; Luchik and Tiederman, 1987). Gao et al. (1989) described these structures in detail for an 18 m tall mixed deciduous forest, and Paw U et al. (1992) for crops and orchards, among other ecosystems. For brevity, turbulent coherent structures will be referred to as "coherent structures", and the term "fluid" will be referred to for either liquid or gases. Negative sensible heat will be defined as the surface and its elements cooling the atmosphere above (i.e., removing sensible heat from the atmosphere), and positive sensible heat, the converse.

2.2.1 Ramp Observations

In common with engineering flows over both smooth and rough surfaces, coherent structures are characterized by repeated temporal and spatial patterns of the velocity and scalar field. Near a surface, where the fluid is assumed to reach zero velocity, a shear zone must be created if the fluid is moving in respect to the surface. It is theorized that the coherent structures are created by the shear. In many engineering flows, the shear zone exists rather extensively above the dimensions of the roughness elements, but in the atmosphere, the shear zone may be the same order of magnitude in extent as the roughness elements. This difference led to the concept that atmospheric coherent structures were analogous to those found in theoretical and laboratory flows called "plane

mixing layers", defined as flows initially starting out as two distinct layers of fluid with different mean speeds, both in parallel directions and in contact with each other at a plane boundary (Raupach et al., 1989, 1996; Paw U et al., 1992).

2.2.2 Turbulent Coherent Structures

Coherent structures are observed to have ejections and sweeps as common features. In an ejection, the near surface fluid, which has characteristics of the near-surface boundary layer, rises upward into the fluid. This is associated with a sweep, as expected from continuity-conservation of mass theory, where fluid farther from the surface, with different characteristics, descends to the near-surface boundary layer. Because of the 'no-slip' condition of zero velocity at the surface, the near-surface fluid is characterized by low horizontal velocities, and if the surface is a scalar source, enhanced scalar values. Conversely, away from the surface that is a scalar source, the fluid is characterized by higher velocity and lower scalar values. Therefore, in an ejection, the fluid has lower horizontal velocity and is moving upward with a positive vertical velocity. In a sweep, faster moving fluid descends rapidly in a gust.

For flows near typical terrestrial ecosystems, plants frequently have a large relatively vertical extent into the atmosphere. The momentum drag created by plant structures slows the air, creating the analogy to a plane mixing-layer. When a coherent structure is formed associated with the mean shear near the plant canopy top, it consists of a linkage of a sweep with at least one ejection. At a single location, a sequence of

ejections and sweeps are observed at an instrumented tower or mast. If the sensible heat flux is positive during the sweep phase, a short-lived rapid horizontal-moving parcel of air gusts into the canopy, bringing cooler air down to the plant elements. In the more quiescent ejection phase, slow horizontal-moving air moves upwards. The ejections are weak near the canopy top (Gao et al., 1989), so the air resides in the canopy sufficiently long to show some heating. This is manifested by a slow temperature rise in the temperature trace with time, and it is terminated by the next gust phase, which causes a sudden temperature drop so the resulting temperature trace exhibits a 'ramp' pattern (Gao et al.,1989, Paw U et al., 1992). Under stable conditions, the pattern is reversed, with a slow temperature drop as the air in the canopy is cooled by the canopy elements, and a sudden temperature rise as a gust brings down the warmer air from above the canopy (Gao et al,.1989, Paw U et al., 1992). Such patterns have been found in the surface layer of the atmosphere and near vegetation by other researchers also (Priestley, 1959; Antonia et al., 1979; Thompson, 1979; Phong-Anant et al., 1980; Wilczak, 1984; Bergstrom and Hogstrom, 1989) and are sometimes associated with gravity (buoyancy) waves (Paw U et al., 1989, 1990)

2.3. Structure Functions and Scalar Ramps

In Paw U et al. (1995), filtering was used to remove scatter and clarify the slow temperature rises and falls associated with plant canopy-atmospheric exchange (Fig. 1); however, because of the necessity to choose filter functions and use numerical methods to identify scalar increases or decreases, this method is cumbersome.

Van Atta (1977) and Antonia and Van Atta (1978) identified the relationship between structure functions, turbulence, and ramp patterns. The structure function, which has been used extensively in turbulence data analysis, is defined as

$$S^n(r) = \frac{1}{m} \sum_{i=1}^{i=m-j} [T(i+j) - T(i)]^n \qquad (1)$$

where m is the number of data points, n is the order of the structure function, j is the sample lag, and i is the data point number. Depending on the sampling frequency (f), the sample lag corresponds to a time lag (r) in seconds. For example, if f = 8 Hz and j=2, then r = 2/8 =0.25 s. Most structure function analysis has concentrated on spatial lags, but because frequently limited instrumentation existed, time lags and the ergodic hypothesis were used to approximate the spatial lags.

Repeated patterns (e.g., ramps in the scalar trace) create special patterns in structure functions, resulting in special relationships between the higher moments. Van Atta (1977) simplified the relationships by making the assumption that ramps were regular patterns of fixed geometry that had instantaneous terminations for unstable conditions, the slow temperature rise would be terminated by an instantaneous temperature drop, and for stable conditions, the slow temperature drop would be terminated by an instantaneous temperature rise. This resulted in a fixed set of probabilities for the structure function values, crucial to the analysis of ramp geometry.

The fixed probabilities are used to determine the ramp dimensions, *a*, the amplitude of the ramp pattern, *s*, the spacing between the sudden temperature drop (or rise) and the beginning of the gradual temperature rise (or drop), and *d*, the duration of the gradual temperature rise or fall as identified in Fig.1. According to the probability analysis the higher order moments of the structure functions are related to the above ramp dimensions in the following manner:

$$S^2 = \frac{a^2 r}{(d+s)}\left[1 - \frac{1}{3}\left(\frac{r}{d}\right)^2\right] \quad (2a)$$

$$S^3 = -\frac{a^3 r}{(d+s)}\left[1 - \frac{3}{2}\left(\frac{r}{d}\right) + \frac{1}{2}\left(\frac{r}{d}\right)^3\right] \quad (2b)$$

$$S^5 = -\frac{a^5 r}{(d+s)}\left[1 - \frac{5}{2}\left(\frac{r}{d}\right) + \frac{10}{3}\left(\frac{r}{d}\right)^2 - \frac{5}{2}\left(\frac{r}{d}\right)^3 + \frac{2}{3}\left(\frac{r}{d}\right)^5\right] \quad (2c)$$

Van Atta (1977) noted that if $r << d$, then the equations can be linearized and a simple set of solutions results in solutions for *a* and $d+s$.

One can determine the ramp dimensions *d* and *s* without the linear assumptions of Van Atta (1977) by using more than one lag, and then using simultaneous solutions, assuming $r < d$ and $r < s$:

$$\frac{S^3(br)}{S^3(r)} = \frac{-\frac{a^3 br}{(d+s)}[1-\frac{3}{2}(b\frac{r}{d})+\frac{1}{2}(b\frac{r}{d})^3]}{-\frac{a^3 r}{(d+s)}[1-\frac{3}{2}(\frac{r}{d})+\frac{1}{2}(\frac{r}{d})^3]} \equiv R \quad (3)$$

If

$$v \equiv \frac{r}{d}$$
$$v^3 - \frac{12-3R}{16-R}v + \frac{4-2R}{16-R} = 0 \quad (3a)$$

which yields a cubic solution for *v* and therefore *d*. The ramp amplitude can be obtained from

$$a^3 + [10S^2(r) - \frac{S^5(r)}{S^3(r)}]\frac{P_3}{P_5}a + 10S^3(r)\frac{P_2}{P_5} = 0 \quad (4)$$

where

$$P_2 = 1 - \frac{1}{3}v^2$$
$$P_3 = 1 - \frac{3}{2}v + \frac{1}{2}v^3$$
$$P_5 = 1 - \frac{5}{2}v + \frac{10}{3}v^2 - \frac{5}{2}v^3 + \frac{2}{3}v^5$$

and *s* is given by

$$s = \frac{-a^3 r}{S^3(r)}P_3 - d \quad (5)$$

Chen et al. (1997a) noted that the ramps observed by Gao et al. (1989) and Paw U et al. (1992) had non-instantaneous terminations. They developed a set of equations to obtain the ramp dimensions, with the assumption that the spacing between ramps (*s*) was zero.

However, now an additional ramp dimension, i.e., the time it takes for the gust to pass by (t_f), is needed (See Fig. 2). Chen et al. (1997a) also noted that equations could be developed for the case when the spacing was non-zero, but they did not present the equations in their articles. From Chen et al. (1997a), the higher order structure functions are predicted to be

$$S^n = (-1)^n \frac{ra^n}{(d+t_f)}\left[(\frac{r}{t_f})^{n-1}(1+\frac{t_f-r}{d}) - \frac{(n-1)}{(n+1)}(\frac{r}{t_f})^2(1-\frac{t_f-r}{d})\right]$$

$$for \quad 0 \le r \le t_f;$$

$$S^n = (-1)^n \frac{ra^n}{(d+t_f)}\left[\frac{(d+t_f-r)^n + (-1)^n(d+t_f-r)r^{n-1}}{d^n}) - \frac{(n-1)t_f(d+t_f)^n f_n}{(n+1)rd^n}\right] \quad (6)$$

$$for \quad t_f < r \le d;$$

$$S^n = \frac{ra^n}{(d+t_f)}\left[\frac{(d+t_f-r)^n}{t_f^{n-1}r}) - \frac{(n-1)(d+t_f-r)^{n+1}}{(n+1)t_f^n r}\right]$$

$$for \quad d < r < d+t_f$$

where

$$f_2 = 1$$

$$f_3 = 1 - 2(\frac{r}{d+t_f})$$

$$f_5 = 1 - \frac{9}{2}(\frac{r}{d+t_f}) + \frac{15}{2}(\frac{r}{d+t_f})^2 - 5(\frac{r}{d+t_f})^3$$

if $r << t_f << d$ then

$$S^2 = \frac{r^2 a^2}{(d + t_f)t_f}$$
$$S^3 = \frac{-r^3 a^3}{2(d + t_f)t_f^2} \quad (7)$$
$$S^5 = \frac{2r^3 a^5}{3(d + t_f)t_f^2}$$

Note that, in Chen et al. (1997a), there was a typographical error for S^5. The important issue here, as noted in Chen et al. (1997a), is that S^n/r approaches zero as r approaches zero, in contrast to the Van Atta (1977) equations, where this ratio approaches a non-zero limit.

In the Chen et al.(1997a) Fig. 7, they showed that the Van Atta (1977) equations are reasonable for S^3/r when $r > 0.1$ s for bare soil (approximately $0.1(d+t_f)$), $r > 0.15$ s for mulch surfaces (approximately $0.15(d+t_f)$), and $r > 1$ s for the forest (approximately $0.05(d+t_f)$). Chen et al. (1997a) reported values of $t_f \approx 0.02$ s to 0.04 s for bare soil, $t_f \approx$ 0.06 s to 0.11 s for mulch, and $t_f \approx 0.18$ s to 0.3 s for the forest. This indicates that when $r > 2t_f$ for tall and $r > 4t_f$ for short canopies, the complete Van Atta (1977) formulations are adequate.

3. Theory of Plant Canopy Surface Renewal

3.1 General Concepts: Volume Energy Budgets

Surface renewal analysis, as used in plant canopies, was originally conceived of as a simple 'transilient' theory (Stull, 1984) in a pseudo-Lagrangian sense (Paw U et al.,

1995). The 'pseudo' part arises because a parcel of air is being followed, but only in a horizontal sense once it is within the plant canopy. The transilience part arises from Stull's concept that turbulent exchange can be described as the exchange of parcels from one known height to another, with weighting factors assigned to the fraction of exchange to one height from each of many other heights. In surface renewal analysis, only two heights are considered, some height above a plant canopy, and a height representing the entire plant canopy. The vertical motions are not followed; however, if one is careful to consider the difference between Eulerian and Lagrangian sources, it can be thought of in an Eulerian sense.

Consider a parcel, which has instantaneously moved down and is now traveling horizontally. As depicted in Fig. 3, under unstable conditions, a ramp will develop if one were to travel with the parcel, and the parcel of air is warmed by the plant canopy elements. In Paw U et al. (1995), the sensible heat flux density during a coherent structure, was derived as:

$$H' = \rho C_p \frac{dT}{dt}\left(\frac{V}{A}\right) \qquad (8)$$

where ρ is the air density, C_p is the specific heat of air, and (V/A) is the ratio of the volume over the horizontal area of the parcel (for a box-shaped parcel, this would be the height of the parcel, and for a parcel in the canopy, then this would be the canopy height). Paw U et al. (1995) noted that the Lagrangian derivative could be written as,

$$\frac{dT}{dt} = \frac{\partial T}{\partial t} + u\frac{\partial T}{\partial x} \qquad (9)$$

If the advective term were close to zero, then the local time derivative would approximate the Lagrangian term. A more complete version of this equation would include the vertical advection term, also, that is,

$$\frac{dT}{dt} = \frac{\partial T}{\partial t} + u\frac{\partial T}{\partial x} + w\frac{\partial T}{\partial z} \qquad (10)$$

Note the axis in the above equation has been aligned with the *x* direction, with the assumption of no cross-longitudinal flow in the *y* direction. Unfortunately, this version is not for a Eulerian but rather for a pseudo-Lagrangian *H*, moving horizontally with the parcel. The difference between the scalar source term in Lagrangian and Eulerian senses is conceived of as a Lagrangian scalar source (S_L) manifested in the change in scalar as the parcel is moving, such as by photochemical or chemical transformation. A Eulerian scalar source (S_e) is manifested in a change in the parcel caused by fixed sources, such as exchange with plant canopy elements. Obviously, it is the latter that is of interest in the estimation of plant canopy exchange processes. The relationship between the two can be derived as following:

$$\frac{dT}{dt} = \frac{\partial T}{\partial t} + u\frac{\partial T}{\partial x} + w\frac{\partial T}{\partial z} = S_L$$

where, based on mass balance into a control volume,

$$\frac{\partial T}{\partial t} + \frac{\partial uT}{\partial x} + \frac{\partial wT}{\partial z} = S_e = \frac{\partial T}{\partial t} + u\frac{\partial T}{\partial x} + w\frac{\partial T}{\partial z} + T(\frac{\partial u}{\partial x} + \frac{\partial w}{\partial z})$$

Therefore,

$$S_e = S_L + T(\frac{\partial u}{\partial x} + \frac{\partial w}{\partial z}) \quad (11)$$

Usually, atmospheric flow is considered incompressible on a micrometeorological scale, so that the two source terms are identical; however, density variations can occur because of scalar fluxes, as embodied in the Webb-Pearman-Leuning correction (Webb et al., 1980), which must be used in conjunction with conservation of mass analysis for exchange analysis in some cases (Paw U et al., 2000), and in such cases there would be a difference between the Lagrangian and Eulerian source terms.

Unpublished data from Li Wang (1999) using large eddy simulation for forest turbulence, and experimental data based on the maize (*Zea mays* L.) experiments described in Paw U et al. (1995), support the notion that in fact the advective terms do approximate zero; however, from Webb et al. (1980) and Paw U et al. (2000), there is a possibility that some correction is needed at times when scalar exchange is estimated using surface renewal analysis because of unaccounted density variations.

Practically, for temperature recorded at the canopy top, the surface renewal equation is expressed as

$$H = \alpha\rho C_p \frac{dT}{dt} h_c . \quad (8a)$$

Here, T is measured at the canopy height, h_c is the canopy height, and α is a calibration factor embodying temperature variation in the canopy initially estimated at 0.5 to account

for a linear change in temperature with height. The time derivative represents the heating during the time period of the ramp only, and during the spacing between ramps, no heating occurs. Any advection or other processes not properly described in surface renewal analysis would also be included in α (Paw U et al., 1995).

3.2 Surface Renewal and Ramps

When the ramp dimensions are determined by structure functions, then the following equation for H_r defines the sensible heat flux density during a ramp.

$$H_r = \alpha\ \rho\ C_p \frac{dT}{dt} h_c \approx \alpha\rho\ \ C_p \frac{\partial T}{\partial t} h_c = \alpha\rho\ \ C_p \frac{a}{d} h_c \qquad (12)$$

When the equation is weighted by the fraction of time that the ramps occur, which is

$\frac{d}{d+s}$, then the sensible heat density is,

$$H = H_r \frac{d}{d+s}, \qquad (13)$$

so

$$H = \alpha\rho C\ \ _p \frac{a}{d} h_c \left[\frac{d}{d+s} \right] = \alpha\rho C\ \ _p \frac{a}{d+s} h_c \qquad (14)$$

Therefore, the linearized Van Atta (1977) equations are sufficient to obtain the sensible heat flux density H (Snyder et al., 1996; 1997). More generally, if the measurements are collected at some arbitrary height z, the equation can be written as,

$$H = \alpha(z)\rho C_p \frac{a}{d+s} z \qquad (15)$$

where α now depends on z.

The concept of different temperature changes (ramp amplitudes) with height leads to the idea of measuring the fast-response temperature change at different heights, and then dividing the canopy into layers whose exchange is represented by these temperature changes. Spano et al. (2000) presented an example. The general equation is,

$$H = \sum_{i=1}^{l} \rho C_p \frac{a(z_i)}{(d+s)_{z_i}} z_i \qquad (16)$$

where l is the number of layers. It is postulated that the factor α is unity and need not be included, the heating is considered constant with height within each layer.

3.3 Surface Renewal and Imperfect Ramps

Chen et al. (1997b) simplified the above equations by starting with Eq.(15), then, using their structure function equation (with finite ramp drop slopes and no quiescent period):

$$\frac{a}{(d+s)^{\frac{1}{3}}} = -\gamma\left[\frac{S^3}{r}\right]^{\frac{1}{3}}$$
$$a = -\gamma\left[\frac{S^3}{r}\right]^{\frac{1}{3}}(d+s)^{\frac{1}{3}} \quad (17)$$

Substituting into Eq. 15, they obtained

$$H = \frac{\alpha\rho C_p z a}{(d+s)} = \frac{-\alpha\rho C_p z\gamma\left[\frac{S^3}{r}\right]^{\frac{1}{3}}(d+s)^{\frac{1}{3}}}{(d+s)} = -\alpha\rho C_p z\gamma\left[\frac{S^3}{r}\right]^{\frac{1}{3}}(d+s)^{-\frac{2}{3}} \quad (18)$$

Based on Raupach et al. (1989), for linearized instabilities,

$$d+s = \frac{h}{\beta u*}; \quad 0.2h_c < z \le h_c + 2(h_c - d_0)$$
$$d+s = \frac{(z-d_0)}{\beta u*}; \quad z > h_c + 2(h_c - d_0) \text{ or } z \le 0.2h_c$$

where d_0 is the zero plane displacement, and α, β and γ are empirical constants. This leads to

$$H = -\alpha\beta^{\frac{2}{3}}\gamma\rho C_p z\gamma\left[\frac{S^3}{r}\right]^{\frac{1}{3}} u*^{\frac{2}{3}} \frac{z}{h_c^{\frac{2}{3}}}; \quad 0.2h_c < z \le h_c + 2(h_c - d_0)$$

$$H = -\alpha\beta^{\frac{2}{3}}\gamma\rho C_p z\gamma\left[\frac{S^3}{r}\right]^{\frac{1}{3}} u*^{\frac{2}{3}} \frac{z}{(z-d_0)^{\frac{2}{3}}}; \quad z > h_c + 2(h_c - d_0) \; or \; z \le 0.2h_c \tag{19}$$

Although Chen et al. (1997b) found some success in using these equations for forest sensible heat flux and the first three factors appeared relatively constant, this method still requires the estimation or measurement of the friction velocity u*, which either requires sonic anemometry or iterative methods.

4. Experimental Comparisons

4.1 Ramp Characteristics in the Canopy

To properly assess surface renewal within plant canopies, one can use the structure method to determine the amplitude and ramp dimension variation with height within the canopy. The general theory noted earlier assumes a linear decrease in amplitude with height and the same ramp repetition frequency. The modified ramp theory limited these assumptions by measuring the ramp amplitude and repetition frequency within the canopy at several heights. Ramp characteristics were estimated using Eqs. 3-5 for three canopies (i.e., maize at 2.6 m height; walnut (*Juglans regia* L.) orchard at 6 m height; mixed deciduous forest at 18 m height). The experimental setup was described in Paw U et al. (1992, 1995).

Amplitude changes with height were not universal curves for all canopies (see Fig. 4). For the forest, irrespective of stability, the amplitude decreased linearly with decreasing height, as originally assumed by Paw U et al. (1995); however, for the maize canopy, the decreasing amplitude is not linear under stable conditions and there was almost no decrease down to 0.2 canopy heights for unstable conditions. The walnut orchard canopy also showed little decrease with height, for either stable or unstable conditions. Since it is not clear how the amplitude will change with height, this implies that the amplitude should be estimated at several heights within a particular canopy.

Surface renewal analysis for H depends on the inverse repetition frequency (d+s). Results for the three canopies showed a universal curve with a decrease in inverse ramp frequency for all three canopies with a decrease of height. The magnitude of d+s was six times longer at 0.2 h_c than at the canopy top (Fig. 5). Stability did not seem to be important for this curve. Equations (3) and (5) help to determine whether the ramp duration (d), the interval between ramps (s), or both change with height. Evidently, the duration d changes little (Fig. 6), whereas s causes much of the change evident d+s (Fig. 7). This indicates that the ramp signal has the same duration throughout the canopy, but not all the ramps, measured at the canopy top, are detected deeper in the canopy. It is possible that not all the coherent structures penetrate deeply into canopies. Only the strongest would reach the bottom. Alternately, the scalar source or sink is not as strong deeper in the canopy. This is supported to some extent by the amplitude variation for the forest. The second hypothesis, however, is not completely supported because one might

expect that even if the scalar source or sink is not so strong deep in a canopy, the interval between ramps should still be similar to that at the canopy top. Irrespective of the details of the canopy turbulence, these results confirm that the surface renewal analysis is more accurate if it is applied over several layers rather than for one layer stretching from the ground surface to the canopy top. It is not possible to determine the above details from the Van Atta (1977) equations, which did not allow *d* or *s* to be obtained individually, nor from Chen et al. (1997a and b), who assumed that $s = 0$.

4.2 Surface Renewal using Van Atta Structure Functions

4.2.1. Raw Data Processing

Several field studies to measure *H* and estimate latent heat flux density (λE) as the residual of the energy balance equation were conducted in recent years (Snyder et al. 1996; Spano et al. 1997a; 1997b; and Spano et al. 2000). In all cases, a structure function analysis from Van Atta (1977) was used to determine the ramp amplitude and inverse ramp frequency. Following the approach of Van Atta (1977), the second, third, and fifth powers of a structure function were used to estimate *a* by solving the third order equation $a^3 + pa + q = 0$ for real roots of the amplitude (*a*), where

$p = 10S^2(r) - \frac{S^5(r)}{S^3(r)}$ and $q = 10S^3(r)$. Then the inverse ramp frequency is calculated as

$d + s = -\frac{a^3 r}{S^3(r)}$. The sensible heat flux density is first estimated, without a correction for unequal heating, as

$$H' = \rho C_p \frac{a}{d+s} z \quad (20)$$

where ρ is the air density, C_p is the specific heat at constant pressure, and z is the measurement height (m). Sensible heat flux density (H_e) was simultaneously measured with a Campbell Scientific, Inc. CA27 (Logan UT), unidirectional sonic anemometer in an eddy covariance system. The Webb et al. (1980) correction was applied to determine the H_e values. Then the surface renewal sensible heat flux density (H), with a correction (α) for unequal heating, was determined by calculating a linear regression through the origin of H_e versus H'. Then H is estimated as

$$H = \alpha H' = \alpha \rho C_p \frac{a}{d+s} z \quad (21)$$

4.2.2. Processed Data

In Snyder et al. (2000) and several other unpublished experiments, high frequency temperature data were not archived in a computer but were processed in a datalogger to output half hour means of the 2nd, 3rd, and 5th order moments of the time lag temperature differences. Then the moments were uploaded and analyzed in a computer to determine the amplitude (a) and inverse ramp frequency ($d+s$) using the Van Atta (1977) structure function methodology. A Campbell Scientific, Inc. CR10x data logger was able to store several months of half hourly net radiation, soil heat flux and structure function moments for two thermocouples using two time lags (i.e., six variables).

In most instances, two 76.2 μm diameter thermocouples were used to measure

temperature. The thermocouples were occasionally broken, but it is unlikely that two were broken at the same time. The thermocouples were mounted at the same height, and a sampling frequency of f=4 Hz was used to collect data. When f=8 Hz was used, the data loggers were unable to make the calculations fast enough to keep up with the sampling and some data were lost; however, it seems that f=4 Hz is sufficiently fast for sampling over most crops. Typically, the time lags r=0.25 and r=0.5 s were used for short canopies and r=0.5 and r=1.0 s were used for taller canopies. The current reading and up to four previous temperature readings (e.g., 0.25, 0.5, 0.75, and 1.0 s earlier) were stored in the data logger using a method similar to registers in a calculator. The procedure to calculate time lag temperature differences and the statistical moments is described below.

If T_4, T_3, T_2, and T_1 were the previous readings taken 1.0, 0.75, 0.5, and 0.25 seconds earlier and T_0 is the current temperature, then, before a new datum was collected, T_4 was overwritten by T_3, T_3 was overwritten by T_2, T_2 was overwritten by T_1, T_1 was overwritten by the previous T_0, and a new value for T_0 was recorded. This was repeated for both thermocouples. Then, using the time lags r=0.5 and r=1.0 s as an example, the differences T_2-T_0 and T_4-T_0, respectively, were temporarily stored. The second, third and fifth moments of the temperature differences were calculated and temporarily stored. At the end of a half hour period, the means of the 2nd, 3rd, and 5th moments were calculated and stored in an output table. For the two thermocouples, there were six mean moments stored.

When using f=4 Hz and time lags r=0.25 and r=0.5 s, it was unnecessary to store the T_4 and T_3 data. Before a new datum was collected, the differences T_1-T_0 and T_2-T_0 were temporarily stored. Then the second, third and fifth moments of the differences were calculated and temporarily stored. At the end of a half hour, the mean moments were calculated and stored in an output table. Again, for the two thermocouples, there were six moments. Because taking the 3rd and 5th power of a fraction can lead to small numbers, the calculations and data storage requires high resolution.

The date and time of the output recording and the six moments were stored in the logger. In addition, net radiation (W m^{-2}) was measured and a soil heat flux plate was placed at 0.04 m depth to measure the heat flux (G_2) in W m^{-2}. These data were collected every five minutes and the half hour means of R_n and G_2 were stored. Temperature above the heat flux plates was recorded with thermocouples at 0.01 and 0.03 m depth at the end of each half hour to estimate soil heat flux density. In the experiments, the change in soil heat storage ΔS is calculated assuming a volumetric heat capacity that correspond to water content near field capacity. The soil heat flux density at the surface is calculated as $G = G_2 + \Delta S$.

The data loggers could usually store 1-2 months of this half hour data, so it provided an easy way to remotely monitor surface renewal and the energy balance. After data were collected, they were processed in a computer. The steps to determine H and λE from the 2nd, 3rd, and 5th moments were described earlier.

4.3. Instrumentation

For surface renewal analysis, high frequency temperature data can be collected using fine-wire thermocouples. Duce et al. (1998) presented the results of an experiment to evaluate the effect of thermocouple characteristics on *SR* analysis. They found that the size and design of sensors used in high frequency measurements does affect temperature traces and *SR* results. Data were collected over a drying bare-soil surface to obtain a wide range of *H* conditions. High frequency (f=8 Hz) temperature data were recorded using exposed 12.7, 25.4, and 76.2 μm diameter single and double wire chromel-constantan thermocouples. Ramp characteristics were determined using the Van Atta (1977) structure function method.

The regression statistics and the root mean square error (RMSE) for H versus H_e and for H' versus H_e are given in Table 1. RMSE values for both uncorrected (H') and corrected (H) surface renewal methods are provided. The α values for unequal heating increased with the both time lag and thermocouple size. Looking at the H' RMSE column, there seems to be little difference in α values resulting from the use of single- or double-wire thermocouples. There was no improvement in accuracy resulting from the use of the 12.7 μm diameter over the 25.4 μm diameter thermocouple. When corrected for unequal heating, the H values are comparable regardless of the thermocouple diameter or the time lag used in the structure function. In fact, the 76.2 μm diameter sensors had the lowest RMSE for H versus H_e, indicating that, when calibrated, the larger sensors give the best estimates of H_e.

The size of the sensor does affect both *a* and *d*+*s*. For example, the 12.7 and 24.5 μm showed bigger ramp amplitudes indicating a more rapid response to fluctuating temperature than the 76.2 μm thermocouples (see Table 1). This in turn affected the third moments of the structure function and hence *d*+*s*.

4.4 Sensor Height and Canopy Type

4.4.1 Tall, Dense Canopies

Differences in the α uneven heating factor, based on structure function time lag (Snyder et al., 1996; Spano et al., 1997b) and on sensor size (Duce et al., 1998) were observed; however, measurement height also can affect the α heating factor (Paw U et al., 1995; Snyder et al., 1996; Spano et al., 1997b, 2000). It is difficult to compare sensor height and canopy type relationships because many of the experiments were conducted using different thermocouple sizes and time lags. In an early paper by Paw U et al. (1995), temperature data were collected over tall canopies including maize, walnut orchard using 12.5 μm diameter sensors and using sonic temperatures over forest. Values of $\alpha \approx 0.5$ were found for each of these canopies when the data were collected at the canopy top. This fit well with the theory of a linear decreasing in heating with depth into the canopies (Paw U et al., 1995). In an experiment, using 76.2 μm thermocouples and 8 Hz sampling over a dense, avocado orchard (*Persea americana* P. Mill.) , Spano et al. (1997b) found a α=0.59 and a decreasing α value above the canopy (Table 2); however, in a similar

experiment, Spano et al. (1997b) reported higher α values for a sparse grapevine canopy (*Vitis* sp.; Table 2). The difference was attributed to deeper penetration by air parcels into the sparser canopy.

4.4.2 Short dense canopies

Snyder et al. (1996), Duce et al. (1997), and Spano et al. (1997b) collected data, using 76.2 μm diameter sensors, at heights well above the top of dense canopies (e.g., grass, wheat (*Triticum aestivum* L.), and sorghum (*Sorghum halepense* L.)). The α values were considerably bigger than reported in Paw U et al. (1995) and they decreased with height above the canopy (Fig.8). Part of the difference between the canopy top and above canopy research was due to sensor size and time lag; however, a measurement height effect was evident in the studies over short dense canopies (Snyder et al., 1996; Spano et al., 1997b) and in and above taller sparse canopies (Spano et al., 2000).

When data were collected at several heights over 0.1 m tall, C-3 species grass using 76.2 μm diameter sensors, Snyder et al. (1996) found poor estimates of H_e from measurements near the canopy top and above 1.0 m height (Fig.8). Good results were obtained for data collected between 0.3 and 0.9 m height. The poor results from the canopy top measurements were attributed to micro-scale advection resulting from measurements too close to the surface. This might have been alleviated using a sampling

frequency greater than 8 Hz. The measurements above 1.0 m were likely in error because the data were collected too far above the canopy and there was likely entrainment of air from above.

Data collected with 76.2 μm diameter sensors at 1.43 times the canopy height over 0.7 m tall wheat provided good RMSE values when surface renewal H was compared with H_e (Spano et al., 1997b, Duce et al., 1997). Results from the canopy top and at 1.86 times the canopy height were less good. The poor results near the canopy top might be due to a fairly high mean wind shear of the horizontal wind (0.93 s^{-1}). Entrainment may have affected readings at the upper height. Spano et al. (1997a,b) also collected data over sorghum, and good results were obtained for 1.0, 1.43, and 1.86 times the canopy height measurements when the time lags were 0.5 and 0.75 s. The results were less good for the 0.25 and 1.0 s time lags. The good estimates of H_e for all heights above the sorghum was attributed to a lower mean wind shear observed for the sorghum (0.68 to 0.45 s^{-1}).

In the studies over grass, wheat and sorghum, the α weighting factor increased with time lag used to calculate the structure function. This is shown in Fig. 9, where the α values from the best measurement height are plotted versus time lag.

4.4.3. Tall, Sparse Canopies

In addition to the trials over dense canopies, experiments were conducted in sparse

grape vineyard canopies near Villasor, Italy and Davis, California (Spano et al., 2000). High frequency (8 Hz) temperature data were collected at several levels within and above the canopy. The foliage was evenly distributed within the upper two thirds of the canopy height (2.2 m) and the ground cover was approximately 65%.

Based on the results of all of the experiments, data collection at about 90% of the canopy height was recommend to provide good estimates of H_e without the need for calibration (Fig. 10). This would give H values with a RMSE of about 45 W m^{-2} of H_E. There was little difference observed between H values coming from the mean of two time lags or four time lags, so using 76.2 μm diameter thermocouples, 8 Hz data, and time lags r=0.25 and 0.50 s yield acceptable performance.

Theoretically, if the volume of air below the measurement height is heated or cooled evenly and other factors are negligible, α =1.0 is expected. In all experiments, the H values overestimated H_e at and above the canopy top measurements (α<1) and underestimated H at heights below the canopy top (α>1). In both cases, a decrease in α with height was obtained. This was consistent with the theory discussed by Paw U et al. (1995) and the results reported in previous experiments (Spano et al, 1997a,b). The α values depend on the temperature measurement level in relation to the postulated height to which the renewal volume was heated or cooled during the ramp event.

When the measurement level is higher than the mean height of the air volume being heated or cooled, entrainment with air aloft could affect the estimate and H values result

in an overestimate (α<1). When the measurement level is lower than the mean height of the air volume being heated or cooled, air above the measurement level within the renewal parcel air is actually heated or cooled but not accounted for in the energy balance in the parcel being considered. Then, H values result in an underestimate of H_e and α will be greater than unity.

4.4.4. Calculation by Layer

Although good estimates of H were possible using data collected at about 90% of the vineyard canopy height, without accounting for uneven heating of the air volume, a method to determine H without calibrating against H_e is desirable. Spano et al. (2000) calculated SR heat flux separately by layer using temperature data measured at the top of each layer, assuming uniform heating within the layer below (Eq. 16). The air heating within the canopy was not uniform, but calculating the heat flux separately by layer and summing over layers provided a good estimate of H without the need for calibration. The canopy was separated into a lower layer from the ground up to approximately the bottom of the foliage (z_1) and an upper layer from that level to the canopy top (z_2-z_1) . The experiment was conducted both in Italy and California.

Calculating H′ by the two layers and summing to obtain the sensible heat flux density (H'), without calibrating, gave estimates of H_e that were similar to using the calibrated H from canopy top measurements (Table 3). Most likely, the air volume below the foliage had uniform heating and the upper layer, containing the foliage, had uniform heating that

was different from the lower layer. When determined separately and summed, the sensible heat flux density estimate was improved over treating the canopy as one layer. Because this eliminates the need for calibration, this approach needs more investigation.

4.5. Examples of Practical Experiments

Evapotranspiration rates for cotton (*Gossypium hirsutum* L.) have been studied extensively with a variety of methods; however, because of changes in the reference evapotranspiration (*ETo*) equations (Walter et al., 2000), better weather station siting, and new cotton varieties, new research is needed to provide the more accurate crop coefficient (*Kc*) values. Although it was not well quantified, growers believed that cotton varieties differ in their *ETc* rates. As a result, an experiment was designed to simultaneous measure *ETc* of two cotton varieties using the surface renewal method.

The temperature data were collected using 76.2 μm diameter sensors at 4 Hz and time lags of 0.25 and 0.50 seconds were used with the structure function (Van Atta, 1977) to determine temperature ramp characteristics. In this field trial, the second, third, and fifth moments of the structure function were calculated and stored in a CR10X data logger. Periodically, the moment data were transferred via phone modem to a computer where $H = \alpha H'$ was calculated. In this experiment, α was determined as the slope of a linear regression through the origin of H_e versus H', where H_e was measured with a CA27 sonic anemometer. Latent heat flux density (*LE=ETc*) was calculated as the residual in the energy balance equation. Figure 11 shows the daily *ETc* calculations for the two

varieties during the season. Note that the thermocouples were replaced once during the season because of corrosion. Damage to the net radiometers and problems with the eddy covariance system were bigger problems than using the thermocouples.

Evapotranspiration rates for rice are believed to be higher than most crops; however, there is questionable evidence for the high rates. As a result, an experiment was designed to simultaneous measure *ETc* of rice using the surface renewal method. The data collection procedure was similar to that used in the cotton experiments. Figure 12 shows the daily *ETc* calculations for rice during the year 2000 growing season. During the growing season, the thermocouples were replaced only once because they were damaged during cultural practices. Again, the net radiometer maintenance and the eddy covariance system were bigger problems the maintaining the thermocouples.

The surface renewal method, using processed data, has been used successfully on a wide range of crops (irrigated pasture, tomatoes (*Solaum lycopersicum* L.), broccoli (*Brassica oleracea* L.), lettuce (*Lactuca* sp.), wheat, sorghum, maize, cotton, citrus and avocado) to determine H and λE as the residual of the energy balance equation. The differences in flux estimates between surface renewal and eddy-covariance is not greatly larger than the differences between eddy-covariances systems themselves (Gaynor and Biltoft, 1989). Because the system is relatively robust and data can be stored in a data logger for long periods of time, it offers a good alternative to Bowen ratio and eddy covariance measurements, which are more expensive and difficult to manage. Since the method is not based on flux gradient theory, the fetch and flat surface requirements that

restrict the use of Bowen ratio and 1-D sonic anemometers may be less of a problem. The method offers a tremendous opportunity for agronomists and engineers to improve evapotranspiration and crop coefficient estimates. It is also a less expensive method to study the effects of water stress on evapotranspiration.

4.6. Other Experiments

Chen et al. (1997b) reported surface renewal analysis using Eq. 19 for bare soil, a straw mulch (both several weeks' data), and a Douglas fir forest (*Pseudotsuga menziesii;* 17 m tall; several days' data), using data gathered at one height. The α values were found to range from 0.47 to 0.69, but did not seem to vary with height for each surface type. Anandakumar (1999) found that the surface renewal method (based on measurements at a single height) predicted sensible heat flux density well when compared to scintillometer estimates, over a 0.9 m tall wheat field, mainly for unstable conditions. The optimum time lag appeared to be 0.3 s, for a measurement height of 1.4 m. He also reported that the ramp repetition frequency and amplitude both appeared important in creating the variation of estimated sensible heat. Katul et al. (1996) used wavelet-filtered signals to obtain surface renewal estimates (for one height-layer), and found agreement with eddy-covariance using one day of 10 Hz data over a loblolly pine (*Pinus taeda* L.) forest.

Castellví et al. (2002) suggested two empirical methods to estimate *H* without calculating the inverse ramp frequency. In one method, the reciprocal of the ramp frequency was estimated as the product of a height parameter, the friction velocity, and a stability function for heat transfer of the surface layer. In the second method, they assumed a linear relationship between the friction velocity and the reciprocal of the ramp period. They found that both of these approaches gave slightly better estimates for *H* than the surface renewal method where the inverse ramp frequency is estimated as a

function of the ramp amplitude. The disadvantage of these methods is that the friction velocity must be measured in addition to high frequency temperature fluctuations.

5. Summary

Surface renewal methods can be used to estimate the exchange of sensible heat, water vapor, and other scalars requiring only scalar traces. In surface renewal, it is assumed that turbulent coherent structures exchange scalars between surfaces and the atmosphere, resulting in ramp structures in the scalar trace. By determining the dimensions of these ramp structures, usually using structure functions, one can estimate the exchange rates. Articles report sensible heat and latent energy errors which generally range from 30 to50 W m^{-2} with some lower and higher values, which are not substantially greater (approximately double) than inter-instrumentation errors using eddy-covariance. Surface renewal methods have worked successfully from surfaces ranging from bare soil to tall forest canopies. If the scalar trace is measured at one height only, a semi-empirical parameter (α) must be determined by comparison of surface renewal results with independently measured exchange rates. This parameter is dependent on height; however, if the scalars are measured at several heights within a plant canopy, the exchange can be estimated without independent determination of the semi-empirical parameter, which can be assumed approximately equal to one under such circumstances. An additional problem which can arise is that the parameter (α) increases somewhat with temperature sensor size, related to a sensitivity of the surface renewal method to slower response scalar sensors.

6. Acknowledgements

Portions of this project were supported by the Office of Science, Biological and Environmental Research Program (BER), U.S. Department of Energy, through the Western Regional Center (WESTGEC) of the National Institute for Global Environmental Change (NIGEC) under Cooperative Agreement No. DE-FC03-90ER61010, and the National Aeronautics and Space Administration SIR-C Shuttle project via the Jet Propulsion Laboratory contract 958445. Dr. Hong-Bing Su helped check some of the derivations and wrote some portions of the computer programs used for part of this Chapter. The authors thank Dr. Sterling Chaykin for supporting a portion of the research at the Satiety Vineyard and Winery in Davis, California and the Consorzio Interprovinciale per la Frutticoltura (Cagliari, Italy) for supporting the research at Villasor, Italy. Other acknowledgements for the experimental data are listed in Paw U et al. (1992) and Paw U et al. (1995).

7. References

Anandakumar, K., 1999. Sensible heat flux over a wheat canopy: optical scintillometer measurements and surface renewal analysis estimations. Agric. For. Meteorol., 96:145-156.

Antonia, R.A. and C.W. Van Atta. 1978. Structure functions of temperature-fluctuations

in turbulent shear flows. J. Fluid Mech. 84:561-580.

Antonia, R.A., A.J. Chambers, C.A. Friehe, and C.W. Van Atta. 1979. Temperature ramps in the atmospheric surface layer. J. Atmos. Sci., 36: 99-108.

Asher, W.E. and J.F. Pankow. 1991. Prediction of gas water mass transport coefficients by a surface renewal model. Environmental Science Technology, 25:1294-1300.

Bergström, H. and U. Högström. 1989. Turbulent exchange above a pine forest. II. Organized structures. Boundary-Layer Meteorol., 49: 231-263.

Bogard, D.G., and W.G. Tiederman. 1986. Burst detection with single-point velocity measurements. J. Fluid Mech., 162: 389-413.

Bogard, D.G., and W.G. Tiederman. 1987. Characteristics of ejections in turbulent channel flow. J. Fluid Mech., 179: 1-19.

Brodkey, R.S., K.N. McKelvey, H.C. Hershey, and S.G. Nychas. 1978. Mass transfer at the wall as a result of coherent structures in turbulently flowing liquid. Int. J. Heat Mass Transfer 21:593-603.

Bullin, J.A. and A.E. Dukler. 1972. Random eddy models for surface renewal: Formulation as a stochastic process. Chem Eng. Sci. 27:439-442.

Castellví, F. and M. Ibañez, and P. J. Perez. 2002. A method based on high frequency temperature measurements to estimate the sensible heat flux avoiding the height dependence. Water Resources Res., in press.

Chen, C-H.P. and R.F. Blackwelder. 1978. Large-scale motion in a turbulent boundary-layer: a study using temperature contamination. J. Fluid Mech., 89: 1-31.

Chen, W., M.D. Novak and T.A. Black. 1997a. Coherent eddies and temperature structure functions for three contrasting surfaces. Part I:Ramp model with finite microfront

time. Boundary-layer Meteorol. 84:99-123.

Chen, W., M.D. Novak and T.A. Black. 1997b. Coherent eddies and temperature structure functions for three contrasting surfaces. Part II: Renewal model for sensible heat flux. Boundary-layer Meteorol. 84:125-147.

Chung, B.T.F., L.T. Fan, and C.L. Hwang. 1971. Surface renewal and penetration models in the transient state. Amer. Indust. Chem. Eng. J. 17:154.

Clayson, C.A., C.W. Fairall, and J.A. Curry. 1996. Evaluation of turbulent fluxes at the ocean surface using surface renewal theory. J. Geophys Res.-Oceans 101(NC12):28503-28513.

Danckwerts, P.V. 1951. Significance of liquid-film coefficients in gas absorption. Indust. Eng. Chem. 43:1460-1467.

Danckwerts, P.V. 1955. Gas absorption accompanied by chemical reaction. Am I. Chem. Eng. J. 1:456.

Denmead, O.T. and I.C. McIlroy. 1970. Measurements of non-potential evaporation from wheat. Agric. Meteorol. 7:285-302.

Denmead, O.T., J.R. Simpson, and J.R. Freney. 1977. A direct field measurement of Ammonia emissions after injection of anhydrous ammonia. Soil Sci. Soc. Amer. J. 41:1001-1004.

Desjardins, R.L. 1972. CO_2 measurements by eddy correlation methods. Bull. Amer. Meteorol. Soc. 53:1040.

Disrud, L.A. and L.T. Fan. 1976. A stochastic model fo rmomentum transfer in wind erosion-a surface renewal concept. In eds. Engelmann, R.J. and G.A. Sehmel, Atmospheric-Surface Exchange of Particulate and Gaseous Pollutants (1974),

Technical Information Center, Office of Public Affairs, Energy Research and Development Administration, Oak Ridge, Tennesee. Pp. 528-539.

Dobbins, W.E. 1956. Nature of oxygen transfer coefficient in aeration systems. In Biological Treatement of Sewage and Industrial Wastes, eds., McCabe J. and W. W. Eckenfelder, Reinhold Publ, New York.

Duce, P., D. Spano, R.L. Snyder, and K.T. Paw U. 1997. Surface renewal estimates of evapotranspiration. Short canopies. Acta Hort. 449, 63-68.

Duce, P., D. Spano, and R.L. Snyder. 1998. Effect of different fine-wire thermocouple design on high frequency temperature measurement. AMS 23rd Conference on Agricultural and Forest Meteorology. Albuquerque, New Mexico, Nov. 2-6, 1998. p. 146-147.

Einstein, H.A. and H. Li. 1956. The viscous sublayer along a smooth boundary. Proc. Amer. Soc. Chem. Eng. J., Eng. Mech. Div. 82:1-27.

Fan, L.T., B.C. Shen, and S.T. Chou. 1993. the surface-renewal theory of interphase transport - a stochastic treatment. Chem. Eng. Sci., 48:3971-3982.

Gao, W., R.H. Shaw, and K.T. Paw U. 1989. Observation of organized structure in turbulent flow within and above a forest canopy. Boundary-Layer Meteorol., 47: 349-377.

Gaynor, J.E. and C.A. Biltoft. 1989. A comparison of two sonic anemometers and fast-response thermometers. J. Atmos. Oceanic Technol., 6: 208-214.

Harriot, P. 1962. A random eddy modification of the penetration theory. Chem Eng. Sci. 17:149-154.

Higbie, R. 1935. The rate of absorption of a pure gas into a still liquid during short periods of exposure. Trans. Am. Inst. Chem. Eng. 31:365-388.

Inoue, E.N., N. Tani, K. Imai, and S. Isobe. 1958. The aerodynamic measurement of photosynthesis over a nursery of rice plants. J. Agirc. Meteool. Tokyo 14:45-53 (Japanese, English summary).

Johansson, A.V. and P.H. Alfredsson. 1982. On the structure of turbulent channel flow. J. Fluid Mech., 122: 295-314.

Katul G., C.I. Hsieh, R. Oren, D. Ellsworth, and N. Phillips. 1996. Latent and sensible heat flux predictions from a uniform pine forest using surface renewal and flux variance methods. Boundary-layer Meteorol. 80:249-282.

Khan, W. 1990. An extension of Danckwerts theoretical surface renewal model to mass transfer at contaminated turbulent interfaces. Mathematical Comp. Model. 14:750-754.

Kline, S.J., W.C. Reynolds, F.A. Schraub, and P.W. Runstadler. 1967. The structure of turbulent boundary layers. J. Fluid Mech., 30: 741-773.

Koltuniewicz A. 1992. Predicting permeate flux in ultrafiltration on the basis of surface renewal concept. J. Membrane Sci. 68:107-118.

Koltuniewicz, A., and A. Noworyta. 1994. Dynamic properties of ultrafiltration systems in light of the surface renewal theory. Ind. Eng. Chem. Res. 33:1171-1179.

Komori, S., H. Ueda, F. Ogino, and T. Mizushina. 1982. Turbulence structure and transport mechanism at the free-surface in an open channel flow. Int. J. Heat Mass Transfer, 25:512-521.

Komori, S., Y. Murakami, and H. Ueda. 1989. The relationship between surface-renewal and bursting motions in an open-channel flow. J. Fluid Mech. 203:103-123.

Koppel, L.B., R.D. Patel, and J.T. Holmes. 1966. Statistical models for surface renewal in

heat and mass transfer: Part I. A.I.Chem. Eng. J. 12:941-946.

Lemon, E.R. 1960. Photosynthesis under field conditions. II. An aerodynamic method for determining the turbulen carbon dioxide exchange between the atmosphere and a cornfield. Agron. J. 52:697-703.

Luchik, T.S. and W.G. Tiederman. 1987. Time scale and structure of ejections and bursts in turbulent channel flows. J. Fluid Mech., 174: 529-552.

Meek, R.L. and A.D. Baer. 1970. The periodic sublayer in turbulent flow. Amer. Indust. Chem. Eng. J. 16:841-848.

Munn, R.E. 1961. Energy budget and mass transfer theories of evaporation. Proc. 2nd Hydrol. Symp. (Toronto), pp.8-30. Cat R32-361/2, Queens Printer, Ottawa, Canada.

Musschenga, E.E., P.J. Hamersma, and J.M.H. Fortuin. 1992. Momentum, heat and mass transfer in turbulent pipe flow - the extended random surface renewal model. Chem. Eng. Sci. 47:4373-4392.

Offen, G.R., and S.J. Kline. 1974. Combined dye-streak and hydrogen-bubble visual observations of a turbulent boundary layer. J. Fluid Mech., 62: 223-239.

Pasquill, F. 1950. Some further considerations of the measurements and indirect evaluation of natural evaporation. Q. J. Roy. Meteorol. Sco. 76:287-301.

Paw U, K.T., R.H. Shaw, T. Maitani, and R. Cionco. 1989. Gravity waves in an almond orchard, Preprints, 19th AMS Conference on Agricultural and Forest Meteorology, March 7-10, Charleston, S.C., 184-185.

Paw U, K.T., R.H. Shaw, and T. Maitani. 1990. Gravity waves, coherent structures and plant canopies, Preprints, 9th AMS Symposium on Turbulence and Diffusion, April 29-May 3, Roskilde, Denmark, 244-246.

Paw U, K.T. and Y. Brunet. 1991. A surface renewal measure of sensible heat flux density. pp. 52-53. In preprints, 20th Conference on Agricultural and Forest Meteorology, September 10-13, 1991, Salt Lake City, Utah. American Meteorological Society, Boston, MA.

Paw U, K.T., Y. Brunet, S. Collineau, R.H. Shaw, T. Maitani, J. Qiu and L. Hipps. 1992. On coherent structures in turbulence within and above agricultural plant canopies. Agric. For. Meteorol. 61:55-68.

Paw U, K. T., J. Qiu, H.B. Su, T. Watanabe, and Y. Brunet. 1995. Surface renewal analysis: a new method to obtain scalar fluxes without velocity data. *Agric. For. Meteorol*., **74**, 119-137.

Paw U, K.T., D.D. Baldocchi, T.P. Meyers, and K. Wilson. 2000. Correction of eddy-covariance measurements incorporating both advective effects and density fluxes. Boundary-layer Meteorol., 97:487-511.

Pence, D.V., D.E. Beasley, and R.S. Figliola. 1994. Heat transfer and surface renewal dynamics in gas-fluidized beds. J. Heat Transfer-Trans. ASME 116:929-937.

Perlmutter, D.D., 1961. Surface renewal models in mass transfer, Chem. Eng. Sci., 16:287-296.

Phillips, L.F. 1992. CO2 transport at the air-sea interface - numerical calculations for a surface renewal model with coupled fluxes. Geophys. Res. Let. 19:1667-1670.

Phong-Anant, D., R.A. Antonia, A.J. Chambers, and S. Rajagopalan. 1980. Features of the organized motion in the atmospheric surface layer. J. Geophys. Res., 85: 424-432.

Priestley, C.H.B. 1959. Turbulent transfer in the lower atmosphere. University of Chicago, Chicago Press, 130 pp.

Pruitt, W.O. 1963. Application of several energy balance and aerodynamic evaporation equations under a wide range of stability. Final Report to USAEPG on contract no. DA-36-039-SC80334. Univ. of California, Davis pp.107-124.

Pruitt, W.O. and F.J. Lourence. 1968. Correlation of climatological data with water requirement of crops. Dept. of Water Sci. and Engr. Paper No. 9001. Univ of California-Davis. 59pp.

Rajagopalan, S. and R.A. Antonia. 1981. Properties of the large structure in a slightly heated turbulent mixing layer of a plane jet. J. Fluid Mech., 105: 261-281.

Raupach, M.R., J.J. Finnigan, and Y. Brunet. 1989. Coherent eddies in vegetation canopies. Proc. Fourth Australasian Conference on Heat and Mass Transfer, Christchurch, New-Zealand, 9-12 May, 75-90.

Raupach, M.R., J.J. Finnigan, and Y. Brunet. 1996. Coherent eddies in vegetation canopies: The mixing-layer analogy. Bound.-Layer Meteorol. 78:251-382.

Shimada, T., S. Omoto, M. Kondo, and K. Fujikawa. 1998. Mass transfer between gases and high viscosity liquids on rotating cylinder with surface renewal action. J. Chem. Eng. Japan 31:273-176.

Snyder, R.L., D. Spano, and K.T. Paw U. 1996. Surface Renewal analysis for sensible and latent heat flux density. Boundary-Layer Meteorol. 77, 249 - 266.

Snyder, R.L., D. Spano, P. Duce, and K.T. Paw U. 1997. Surface renewal estimates of evapotranspiration. Theory. Acta Hort. 449, 63-68.

Snyder, R.L., K. Bali, F. Ventura, and H. Gomez-MacPherson. 2000. Estimating evaporation from bare or nearly bare soil. J. of Irrig. & Drain. Eng. 126 (6): 399-403.

Soloviev, A.X., and P. Schlussel. 1994. Parameterization of the cool skin of the ocean and of the air ocean gas transfer on the basis of modeling surface renewal. J. Phys. Ocean. 24:1339-1346.

Spano, D., P. Duce, R.L. Snyder, and K.T. Paw U. 1997a. Surface renewal estimates of evapotranspiration. Tall canopies. Acta Hort. 449, 63-68.

Spano, D., R.L. Snyder, P. Duce, and K.T. Paw U. 1997b. Surface renewal analysis for sensible heat flux density using structure functions. Agric. For. Meteorol. 86, 259 - 271.

Spano, D., R.L. Snyder, P. Duce, and K.T. Paw U. 2000. Estimating sensible and latent heat flux densities from grapevine canopies using surface renewal. Agric. Forest Meteorol. 104:171-183

Stull, R.B. 1984. Transilient turbulence theory. 1. The concept of eddy-mixing across finite distances. J. Atmos. Sci. 41:3351-3367.

Stull, R.B. 1988. An introduction to boundary layer meteorology. Kluwer Academic Publishers, 666 pp.

Sutton, O.G. 1953. Micrometeorology. McGraw-Hill, New York, 333pp.

Swinbank, W.C. 1951, Measurement of vertical transfer of heat and water vapor by eddies in the lower atmosphere. *J. Meteorol*., **8,** 135-145.

Swinbank, W.C. 1955*, Eddy transports in the lower atmosphere*. Tech. Paper No. 2, Division of Meteorological Physics, Commonwealth Scientific and Industrial Research Organization, Melbourne, Australia. 30pp

Talmon, A.M., J.M.G. Kunen, and G. Ooms. 1986. Simultaneous flow visualization and Reynolds-stress measurement in a turbulent boundary layer. J. Fluid Mech., 163: 459-

478.

Tanner, C.B. 1960. Energy balance approach to evapotranspiration from crops. Soil Sci. Soc. Am. Proc. 24: 1-9.

Thompson, N. 1979. Turbulence measurements above a pine forest. Boundary-Layer Meteorol., 16: 293-310.

Thorthwaite, C.W. and B. Holzman. 1942. Measurement of evaporation from land and water surface. USDA Tech. Bull. 817: 1-75.

Torr, H.L., and J.M. Marchello. 1958. Film-penetration model for mass and heat transfer. Amer. Indust. Chem. Eng. J. 4:97-101.

Van Atta, C.W., 1977. Effect of coherent structures on structure functions of temperature in the atmospheric boundary layer. Arch. of Mech. 29, 161-171.

Verma, S.B., N.J. Rosenberg, and B.L. Blad. 1978. Turbulence exchange coefficients for sensible heat and water vapor under advective conditions. J. Appl. Meteorol. 17:330-338.

Walter, I.A., R.G. Allen, R. Elliott, M.E. Jensen, D. Itenfisu, B. Mecham, T.A. Howell, R. Snyder, P. Brown, S. Eching, T. Spofford, M. Hattendorf, R.H. Cuenca, J.L. Wright, D. Martin. 2000. ASCE's Standardized Reference Evapotranspiration Equation. Proc. of the Watershed Management 2000 Conference, June 2000, Ft. Collins, CO, American Society of Civil Engineers, St. Joseph, MI.

Webb, E.K., G.I. Pearman, and R. Leuning. 1980. Correction of flux measurements for density effects due to heat and water vapour transfer. Q. J. R. Meteorol. Soc. 106, 85 - 100.

Wilczak, J.M. 1984. Large-scale eddies in the unstably stratified atmospheric surface layer.

Part I: Velocity and temperature structure. J. Atmos. Sci., 41: 3537-3550.

Yoon, K.H., and O.O. Park. 1994. Analysis of a reactor with surface renewal for poly(ethylene terephthalate) synthesis. Polymer Eng. Sci. 34:190-200

Yoon, K.H., and O.O. Park. 1995. Diffusion of butanediol in poly(butylene terephthalate) (pbt) melt and analysis of pbt polymerization reactor with surface renewal. Polymer Eng. Sci. 35: 703-708.

Yuan, T.D. and J.A. Liburdy. 1992. Application of a surface renewal model to the prediction of heat transfer in an impinging jet. Int. J. Heat Mass Transfer 35:1905-1912.

Zappa, C.J., A.T. Jessup, and H. Yeh. 1998. Skin layer recovery of free-surface wakes: Relationship to surface renewal and dependence on heat flux and background turbulence. J. Geophys. Res., 103(NC10):21711-21722.

Zudin, Y.B. 1993. Calculation of turbulent friction and heat exchange using a modified model of surface renewal. High Temperature, 31:710-716. V116(N4):929-937.

Table 1. Statistics for linear regressions through the origin for H_e versus H' by time lag and thermocouple size. RMSE values are for both H' and H versus H_e.

Tcs	time lag (s)	α	R^2	H′ - RMSE (W m^{-2})	H – RMSE (W m^{-2})	N
	0.25	1.04	0.54	37	36	66
25.4 μm	0.50	1.23	0.49	44	38	65
Single	0.75	1.38	0.47	51	39	66
Wire	1.00	1.53	0.43	57	40	61
	0.25	1.60	0.57	57	35	67
76.2 μm	0.50	1.61	0.57	57	35	67
Single	0.75	1.70	0.48	62	38	67
Wire	1.00	1.90	0.38	68	41	64
	0.25	0.90	0.46	40	38	64
12.7 μm	0.50	1.07	0.40	41	40	63
Double	0.75	1.19	0.21	50	46	63
Wire	1.00	1.29	0.08	55	49	61
	0.25	1.04	0.50	37	37	64
25.4 μm	0.50	1.18	0.43	43	39	63
Double	0.75	1.32	0.38	50	41	62
Wire	1.00	1.42	0.37	53	40	59
	0.25	1.88	0.59	66	33	64
76.2 μm	0.50	1.92	0.59	68	33	64
Double	0.75	2.00	0.57	70	34	64
Wire	1.00	2.13	0.53	73	36	62

Table 2. Statistics for linear regressions through the origin for H_e versus H' by measurement height, where α is the slope, for grapevines (*Vitis* sp.) and avocados (*Persea Americana* P. Mill.). RMSE values are for H' and H versus H_e.

Crop	z	α	R^2	H - RMSE	H′ - RMSE	N
	(m)			(W m^{-2})	(W m^{-2})	
Grapevine	2.00	0.87	0.79	49	38	33
Grapevine	2.30	0.80	0.71	68	44	35
Grapevine	2.60	0.74	0.72	82	43	35
Grapevine	2.90	0.65	0.79	115	38	35
Avocado	5.15	0.59	0.69	85	36	40
Avocado	5.45	0.46	0.54	145	42	36
Avocado	5.75	0.30	0.73	287	33	36
Avocado	6.05	0.27	0.72	314	34	40

Table 3. Statistics for linear regressions through the origin for H_e versus H' using two time lags r=0.25 and 0.50 s from data collected at Villasor, Italy and at the Satiety vineyards in Davis, CA. H' was determined as the sum of two layers where the lower layer was from the ground up to the bottom of the foliage and the upper layer included all the foliage.

Location	α	R^2	RMSE	N
			($W\ m^{-2}$)	
Villasor, Italy	0.93	0.90	32	89
Davis, CA	1.05	0.87	42	298

FIGURE CAPTIONS

Fig. 1. Idealized scalar ramp trace and probability (***P(dT)***) of structure function values (***dT***). ***a*** is the scalar amplitude, ***d*** is the duration, ***s*** is the separation between the end of one ramp the commencement of another, ***T*** is the scalar value or concentration, and ***dT*** is the difference in the scalar ***T*** between one time and another time lagged by ***r***.

Fig. 2. Scalar ramp trace with non-infinite drop, after Chen et al. (1997a). ***a*** is the scalar amplitude, ***d*** is the duration (until the drop), and t_f is the duration of the drop; note there is no separation between ramps, so "***s***" is zero and therefore is not shown.

Fig. 3. Cartoon of surface renewal process. Parcel instant drops from position 1 to position 2 in the canopy (upper cartoon). Scalar starts increasing in the parcel because of a source in the canopy, shown in the scalar ***T*** versus time plot (lower graph). After horizontally advecting some distance, the parcel instantly rises from position 3 to position 4 (upper cartoon). The scalar has continued to increase to a peak corresponding to position 3, in the scalar versus time plot (lower graph). Simultaneously, from position 5, a new parcel instantly replaces the old parcel's location in the canopy, shown as position 6 (offset horizontally in the upper cartoon for clarity). This results in an instant drop in the scalar value (lower graph), terminating the previous gradual scalar increase and forming the ramp pattern.

Fig. 4 Ramp amplitude variation determined by structure functions within a canopy. Circles are for the maize canopy, triangles for the walnut orchard, and squares for the forest. Open symbols depict unstable conditions, closed symbols, stable conditions. The vertical axis is height normalized to the canopy height, and the horizontal axis is the amplitude at any height normalized to the amplitude at the canopy top.

Fig. 5 Inverse ramp repetition frequency ($d+s$) variation determined by structure functions within a canopy. Circles are for the maize canopy, triangles for the walnut orchard, and squares for the forest. Open symbols depict unstable conditions, closed symbols, stable conditions. The vertical axis is height normalized to the canopy height, and the horizontal axis is $d+s$ at any height normalized to that at the canopy top.

Fig. 6 Ramp duration d variation determined by structure functions within a canopy. Circles are for the maize canopy, triangles for the walnut orchard, and squares for the forest. Open symbols depict unstable conditions, closed symbols, stable conditions. The vertical axis is height normalized to the canopy height, and the horizontal axis is the duration d at any height normalized to that at the canopy top.

Fig. 7 Ramp spacing duration s variation determined by structure functions within a canopy. Circles are for the maize canopy, triangles for the walnut orchard, and squares for the forest. Open symbols depict unstable conditions, closed symbols, stable conditions. The vertical axis is height normalized to the canopy height, and the horizontal axis is the spacing s at any height normalized to that at the canopy top.

Figure 8. Weighting factor (α) for grass, wheat, and sorghum averaged over time lags r=0.25, 0.5, 0.75, and 1.0 s versus height expressed as the measurement height over the canopy height (z/h_c).

Figure 9. Weighting factor (α) for grass, wheat, and sorghum versus time lag for the best measurement height.

Figure 10. Weighting factor (α) versus height expressed as the measurement height over the canopy height (z/h_c) for a 2.2 m tall, grape vineyard with hedge-row trellising.

Figure 11. Daily crop evapotranspiration (ET_c) data for Pima and Upland cotton during the year 2000 growing season. Cotton evapotranspiration was estimated as the residual of the energy balance equation and H measured using the surface renewal method.

Figure 12. Rice evapotranspiration (ET_c), reference evapotranspiration (ET_o) and rice crop coefficient (K_c) from a field trial near Nicolaus, California. Rice evapotranspiration was estimated as the residual of the energy balance equation and H measured using the surface renewal method.

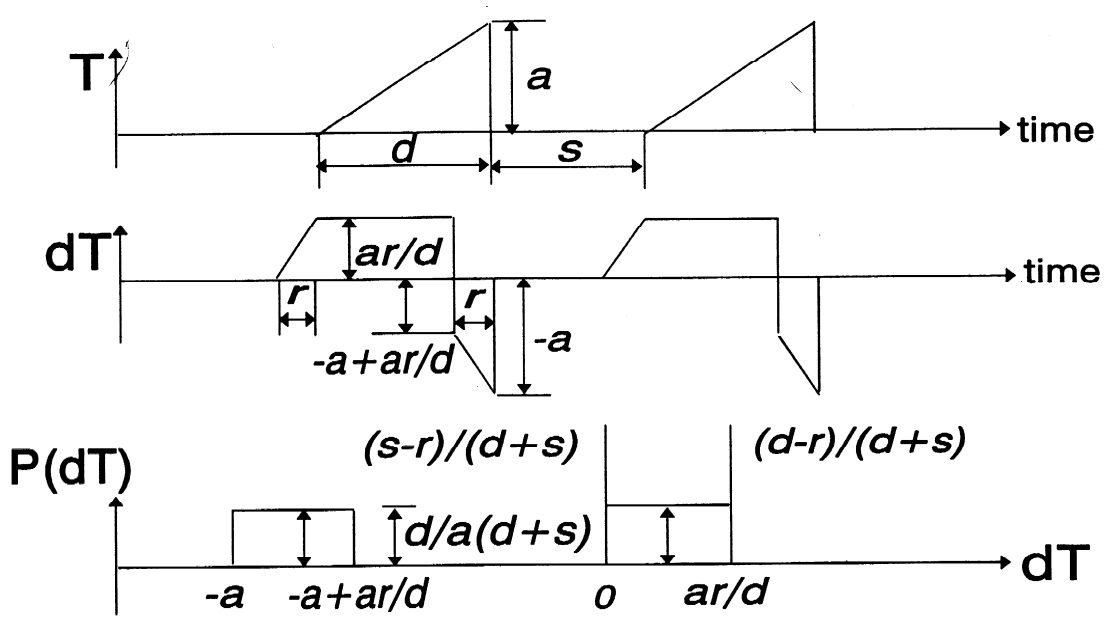
T
a
time
d
s
dT
ar/d
time
r
r
-a
-a+ar/d
P(dT)
(s-r)/(d+s)
(d-r)/(d+s)
d/a(d+s)
dT
-a
-a+ar/d
o
ar/d

Fig. 1.

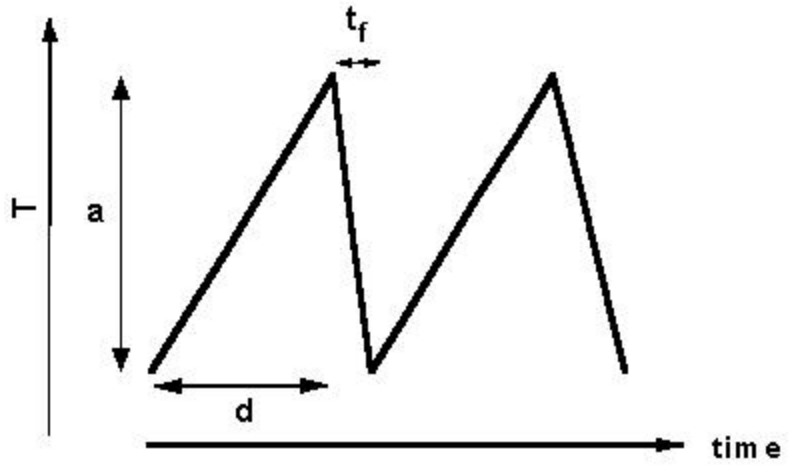

Fig. 2.

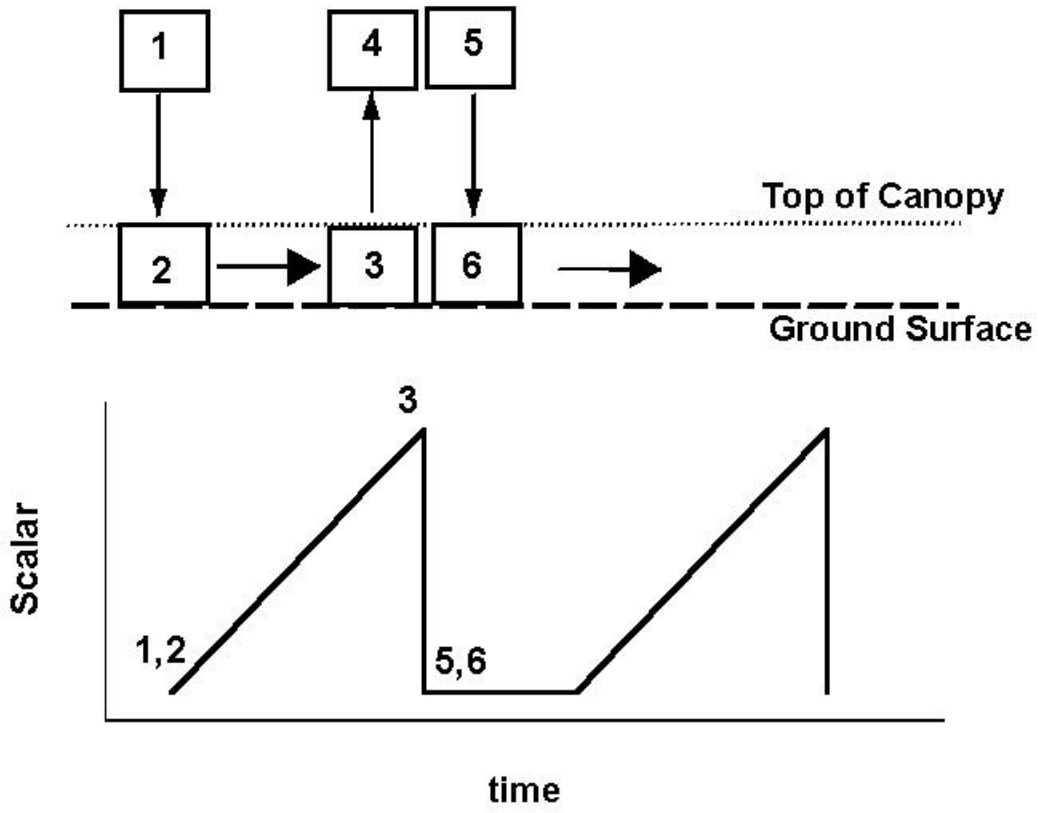

Figure 3.

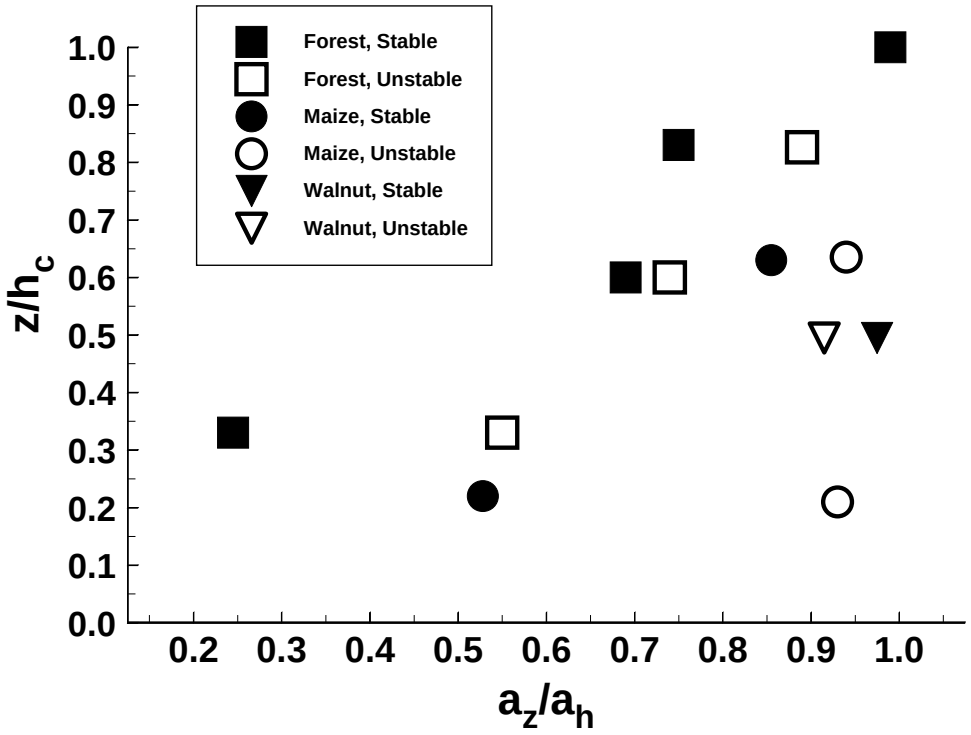
Forest, Stable
Forest, Unstable
Maize, Stable
Maize, Unstable
Walnut, Stable
Walnut, Unstable
1.0
0.9
0.8
0.7
0.6
0.5
0.4
0.3
0.2
0.1
0.0
z/h_c
0.2
0.3
0.4
0.5
0.6
0.7
0.8
0.9
1.0
a_z/a_h

Fig. 4.

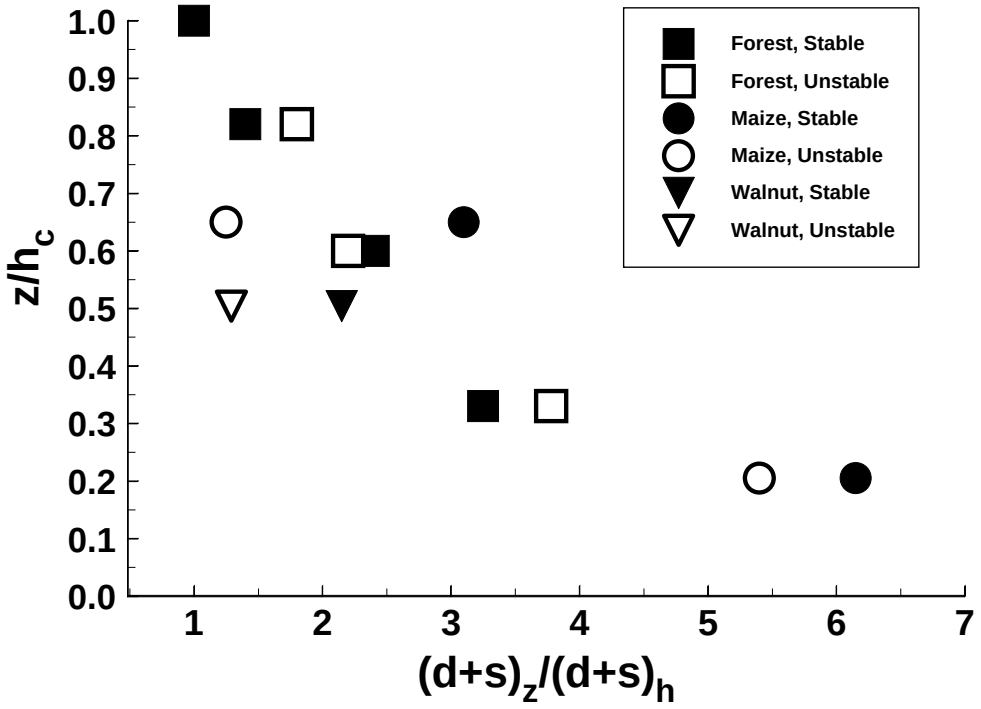
1.0
0.9
0.8
0.7
0.6
0.5
0.4
0.3
0.2
0.1
0.0
z/h_c
1
2
3
4
5
6
7
(d+s)_z/(d+s)_h
Forest, Stable
Forest, Unstable
Maize, Stable
Maize, Unstable
Walnut, Stable
Walnut, Unstable

Fig. 5.

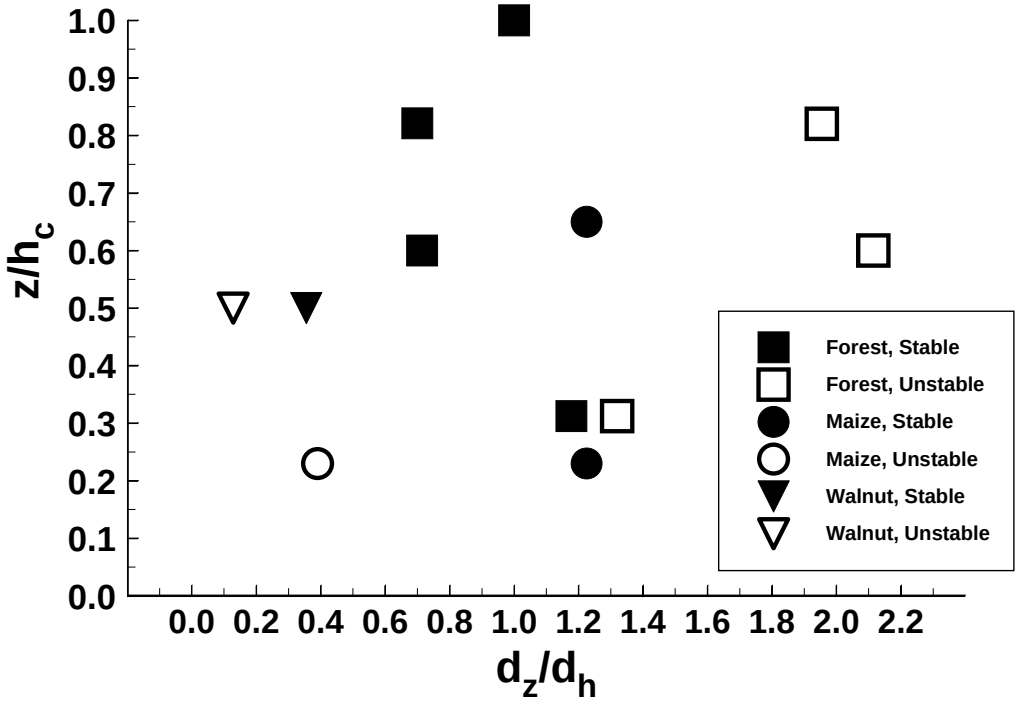
1.0
0.9
0.8
0.7
0.6
0.5
0.4
0.3
0.2
0.1
0.0
z/h_c
0.0 0.2 0.4 0.6 0.8 1.0 1.2 1.4 1.6 1.8 2.0 2.2
d_z/d_h
Forest, Stable
Forest, Unstable
Maize, Stable
Maize, Unstable
Walnut, Stable
Walnut, Unstable

Fig. 6.

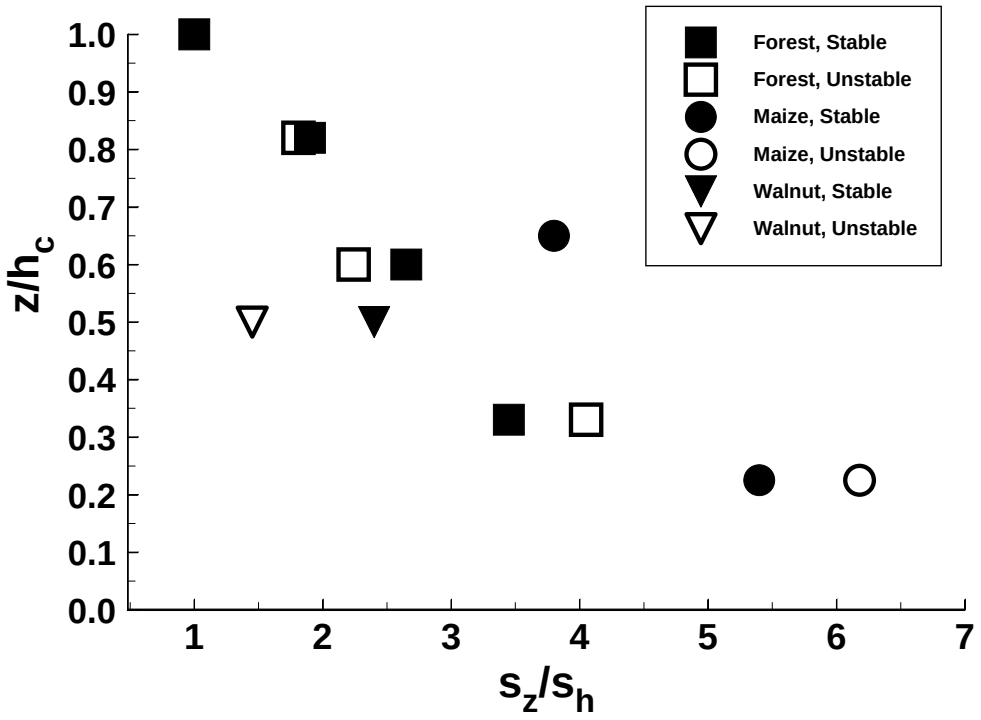
Forest, Stable
Forest, Unstable
Maize, Stable
Maize, Unstable
Walnut, Stable
Walnut, Unstable
z/h_c
s_z/s_h
0.0
0.1
0.2
0.3
0.4
0.5
0.6
0.7
0.8
0.9
1.0
1
2
3
4
5
6
7

Fig. 7.

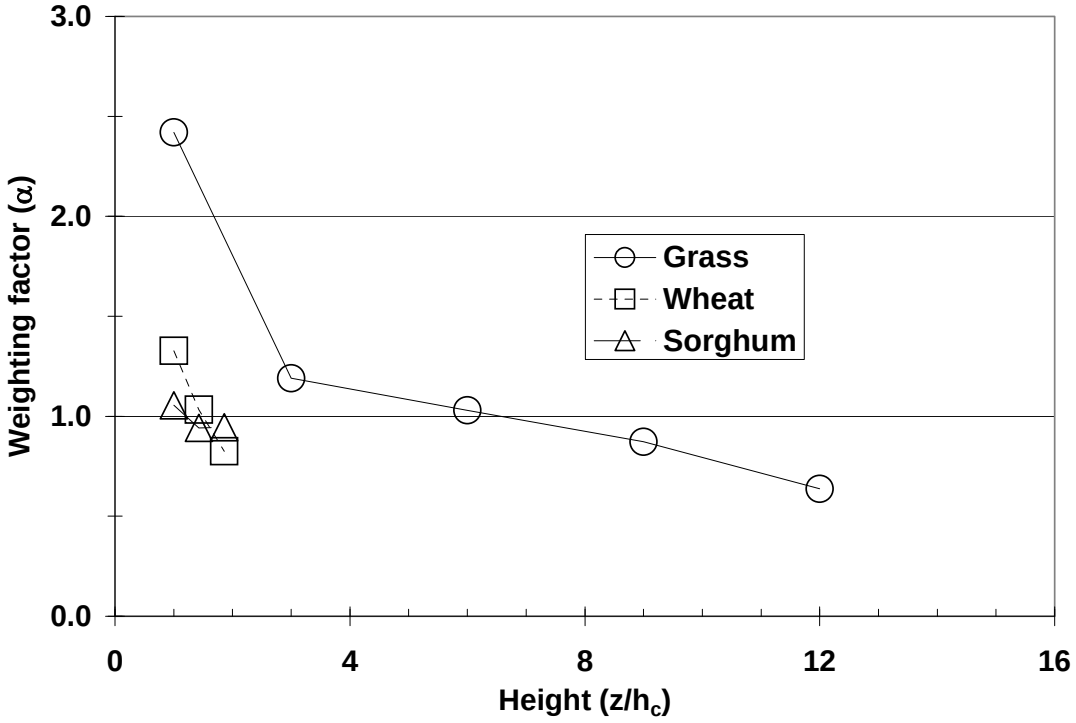
3.0
2.0
1.0
0.0
Weighting factor (α)
0
4
8
12
16
Height (z/h_c)
Grass
Wheat
Sorghum

Figure 8.

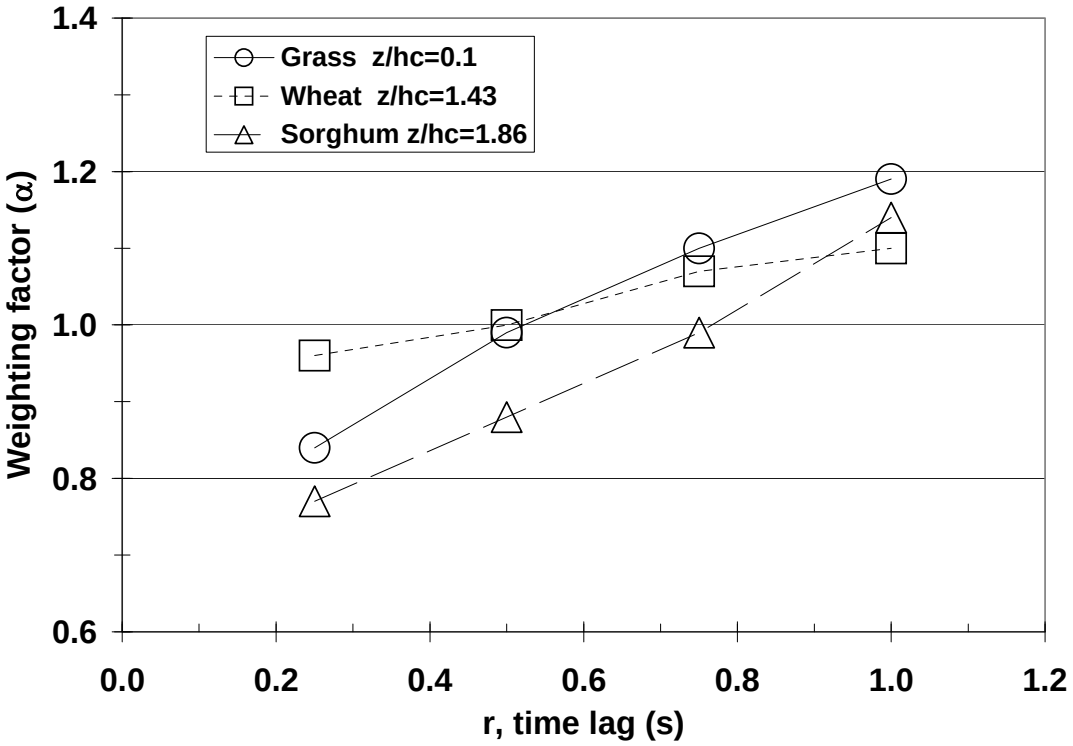
Grass z/hc=0.1
Wheat z/hc=1.43
Sorghum z/hc=1.86
Weighting factor (α)
r, time lag (s)
1.4
1.2
1.0
0.8
0.6
0.0
0.2
0.4
0.6
0.8
1.0
1.2

Figure 9.

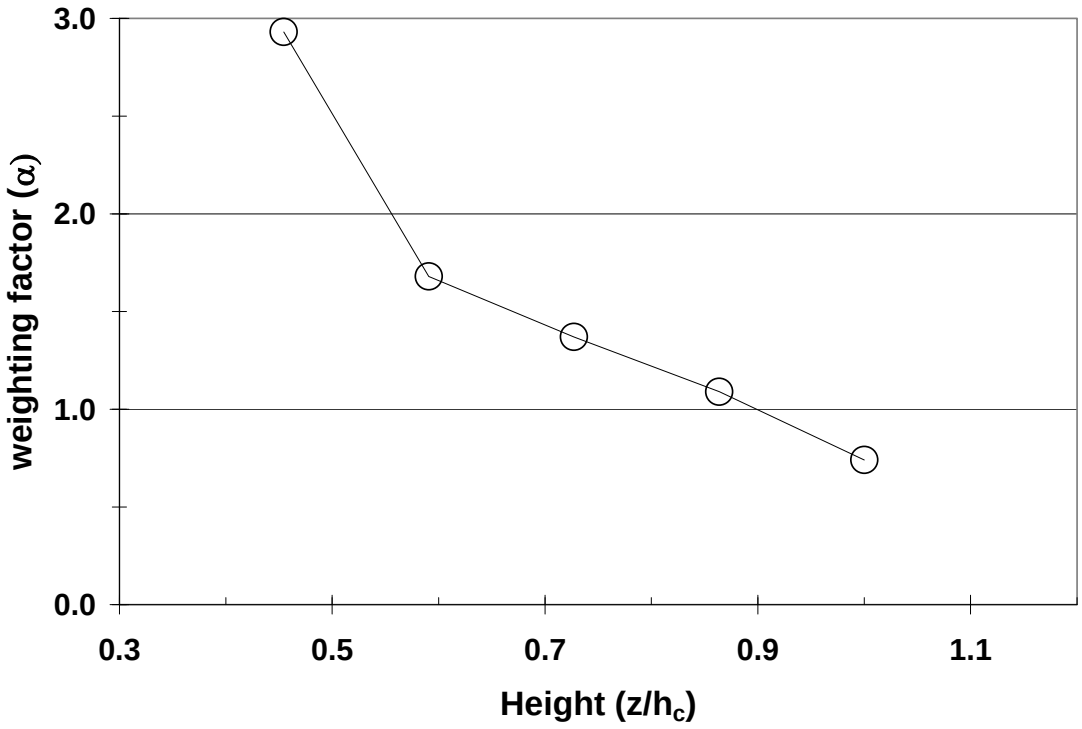

Figure 10.

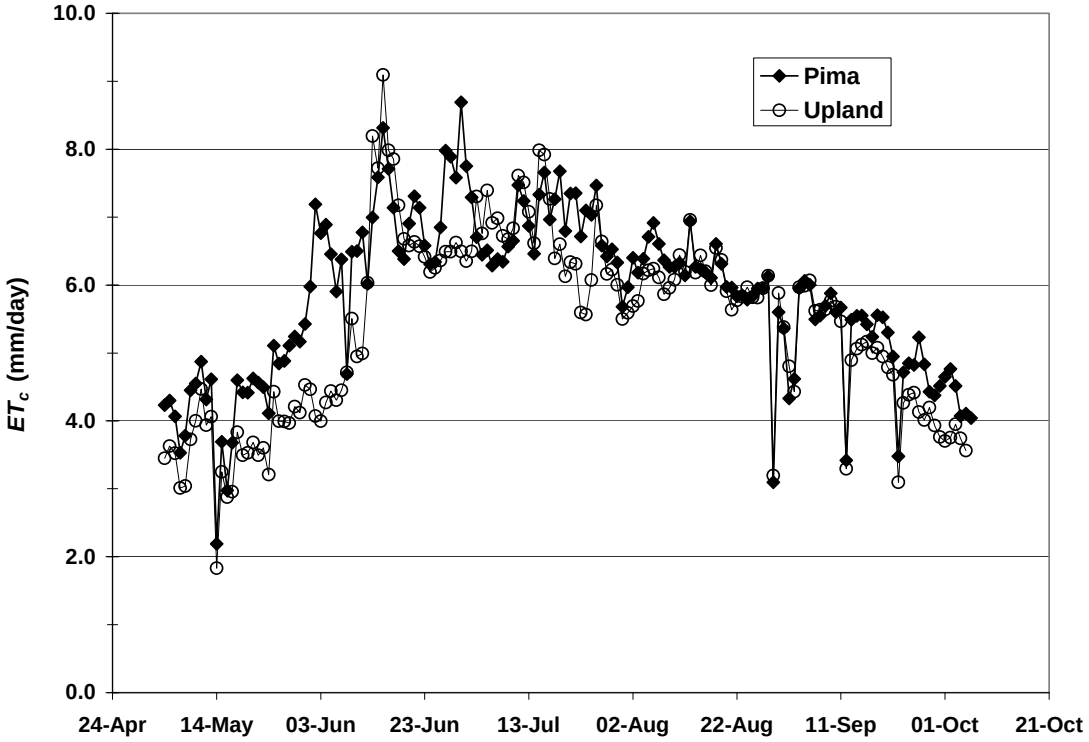
10.0
8.0
6.0
4.0
2.0
0.0
ETc (mm/day)
Pima
Upland
24-Apr
14-May
03-Jun
23-Jun
13-Jul
02-Aug
22-Aug
11-Sep
01-Oct
21-Oct

Figure 11.

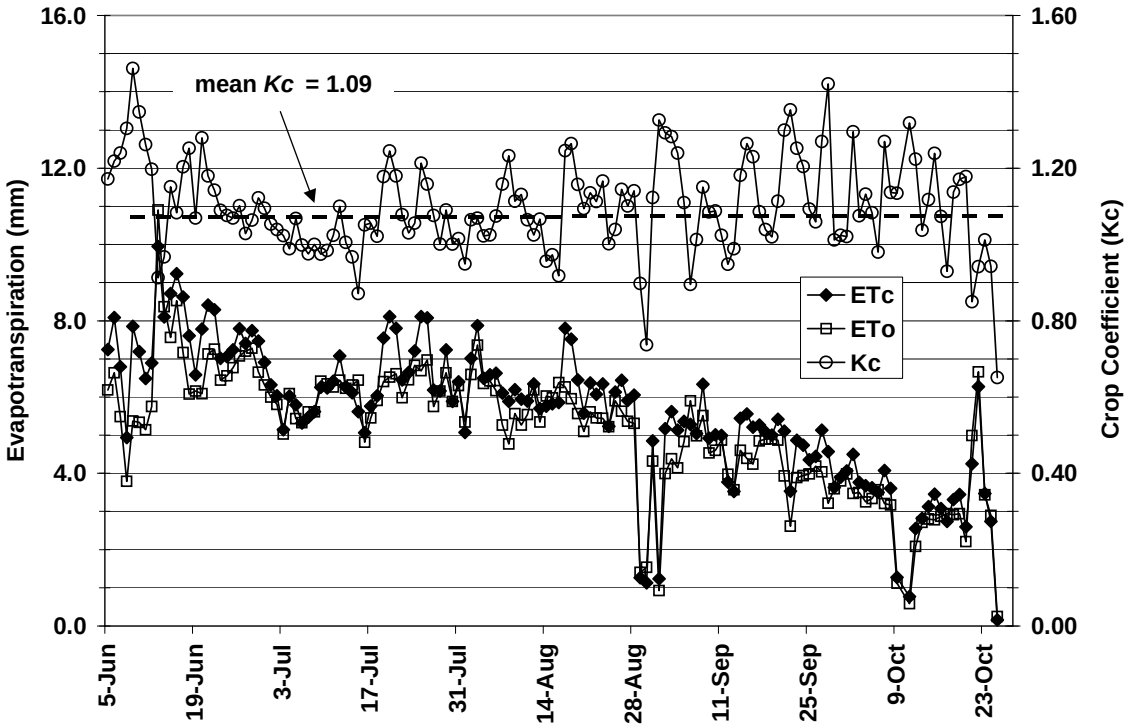
16.0
12.0
8.0
4.0
0.0
1.60
1.20
0.80
0.40
0.00
Evapotranspiration (mm)
Crop Coefficient (Kc)
mean Kc = 1.09
ETc
ETo
Kc
5-Jun
19-Jun
3-Jul
17-Jul
31-Jul
14-Aug
28-Aug
11-Sep
25-Sep
9-Oct
23-Oct

Figure 12.